Strong spin-lattice coupling in multiferroic hexagonal manganite YMnO$_3$ probed by ultrafast optical spectroscopy

Kyeong-Jin Jang,[1] Han-gyoel Lee,[1] Sangkyung Lee,[1] Jaewook Ahn,[1,a] Jai Seok Ahn,[2,b]
Namjung Hur,[3] and Sang-Wook Cheong[4]

[1]*Department of Physics, Korea Advanced Institute of Science and Technology, Daejeon 305-701,
Republic of Korea*
[2]*Department of Physics, Pusan National University, Pusan 609-735, Republic of Korea*
[3]*Department of Physics, Inha University, Incheon 402-751, Republic of Korea*
[4]*Department of Physics and Astronomy, Rutgers Center for Emergent Materials, Rutgers University,
Piscataway, New Jersey 08854, USA*

We report the observation of spin-lattice coupling in multiferroic YMnO$_3$ by femtosecond near-infrared pump and probe spectroscopy. A coherent 31 GHz acoustic phonon was detected above the magnetic ordering temperature, and a higher frequency coherent mode was observed in the antiferromagnetic phase. This temperature-dependent measurement demonstrates that the acoustic phonon excitation is coupled to spin ordering. © *2010 American Institute of Physics.*
[doi:10.1063/1.3467459]

Magnetic material studies for modern electronics have focused on multifunctional properties aimed toward developing high-density, nonvolatile, and energy nonconsuming mass-information storage.[1] In particular, multiferroic materials, which simultaneously exhibit ferroelectricity and ferromagnetism, or at least some kind of magnetic ordering, have been brought to the fore, because of the possibility of controlling magnetic properties with electric fields and the dielectric properties by magnetic fields.[2,3] For a multiferroic system, spin fluctuations can cause unusual dynamic effects, due to strong spin-lattice coupling. Thus, time-resolved optical studies can directly investigate the coupled dynamics between spin and lattice for both fundamental physics and practical applications.[4,5]

YMnO$_3$ in its hexagonal phase is one of the few multiferroic materials where ferroelectric and antiferromagnetic ordering coexist.[6] For a multiferroic system with geometrically frustrated magnets, spin fluctuations can cause unusual dynamic effects, due to strong spin-lattice coupling. In particular, in the vicinity of the magnetic phase transition, the generation of coherent phonons and their time-dependent analysis can be used to study the coupled dynamics of spin and lattice.[7] Regarding the multiferroic properties, there have been many studies of the crystallography, optical properties, and magnetic structural changes.[6,8,9] However, the interrelationships are still far from completely understood. Temperature-dependent studies have provided a better understanding of magnetoelectric coupling;[10–12] in particular, spin-lattice coupling has been observed in measurements of linear optical responses and thermal conductivity as well as in neutron diffraction studies.[13,14] Time-dependent studies are expected to complement conventional optical methods. In this regard, pump-probe methods of time-resolved optical spectroscopy have been widely used to investigate nonequilibrium states of electron, phonon, and spins in manganese oxide materials; they have also been useful in discovering the

physical properties of correlated-electron materials.[15]

In this letter, we present a femtosecond pump-probe reflection measurements of YMnO$_3$ in the temperature range 10–300 K. YMnO$_3$ has a ferroelectric phase transition at T_c >900 K and an antiferromagnetic phase transition at T_N ≃80 K.[16] We investigated the dynamics of optically induced lattice vibrations in the vicinity of the antiferromagnetic phase transition. A coherent 31 GHz acoustic phonon was detected above the magnetic ordering temperature, and a higher frequency coherent mode was observed in the antiferromagnetic phase. Time-resolved measurements over a wide range of temperatures revealed that the coherent acoustic phonon was coupled to the magnetic ordering.

YMnO$_3$ single crystals were grown using a flux method. The *ab*-plane sample was cleaved as a ∼100 μm thick platelet. We noted that a small mosaic spread, formed on the surface of the crystal, was composed of grains with an order of ∼100 μm; see Fig. 1(a). The sample was characterized by x-ray diffraction (XRD) using Cu $K\alpha$ radiation. Figure 1(b) shows the XRD measurement of the *c*-cut sample where the (004) peak at 31° and the (006) peak at 48° are identified. We also examined the crystal with a JEOL JEM-3010 high-resolution transmission electron microscope, operating at 300 kV. The diffraction spots in Fig. 1(c) are indexed using hexagonal unit-cell notation, according to the crystal structure of YMnO$_3$. A high-resolution [001]-zone image is shown in Fig. 1(d).

The time-resolved reflectance measurement of the sample was carried out using fast-scanning pump-probe spectroscopy. The sample was first pumped by a 50-fs short pulse from a Ti:sapphire laser oscillator, operated at an 80 MHz repetition rate. The photon energy of the laser for both pump and probe was ∼1.59 eV, close to the resonant Mn *d-d* transition of YMnO$_3$.[17] The resonance electronic transition was $d_{(x^2-y^2)',(xy)'} \rightarrow d_{(3z^2-r^2)'}$ and the occupied $d_{(3z^2-r^2)'}$ orbital is responsible for the short range antiferromagnetic correlation.[18] The optical reflectivity of a probe pulse was then measured as a function of the time delay between the pump and probe. To produce a time delay between the two pulses, a raster scanning shaker (APE Scan Delay) was in-
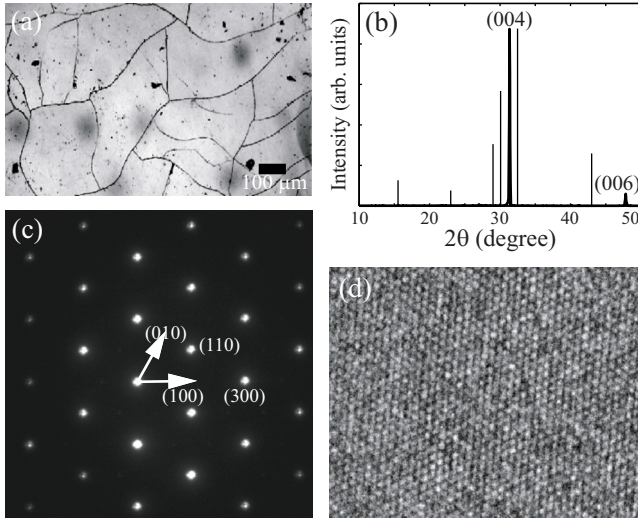
FIG. 1. (Color online) (a) Mosaic spread on the sample surface. (b) X-ray diffraction pattern of $YMnO_3$ with Cu $K\alpha$ radiation at room temperature. The sample was grown along the c-axis. (c) [001]-zone axis electron diffraction pattern of $YMnO_3$. (d) [001]-zone high-resolution transmission electron microscope image.

serted in the path of the pump pulse. The focused spot sizes of the pump and probe pulses at the sample were ~ 80 μm and 50 μm, respectively. Local heating of the sample was minimized by reducing the pump laser fluence below 20 $\mu J/cm^2$. The pump beam polarization was set perpendicular to the probe beam to eliminate both coherent artifacts and scattered pump noise. The sample temperature was varied from 10 to 300 K with a liquid He-filled cryostat (JANIS ST-500).

The measured $YMnO_3$ photoinduced reflectance change $\Delta R/R$ is shown in Fig. 2. Data are plotted as a function of time-delay at various sample temperatures to show the coherent oscillatory changes in the reflectance and relaxation behavior. The oscillation period in the low temperature range below T_N was different from that in the high region. Fourier-transform (FT) analysis was used to extract frequency domain information from the reflectance oscillations. The FT results are shown in Fig. 3 as a two-dimensional intensity plot as a function of frequency and temperature. Two strik-
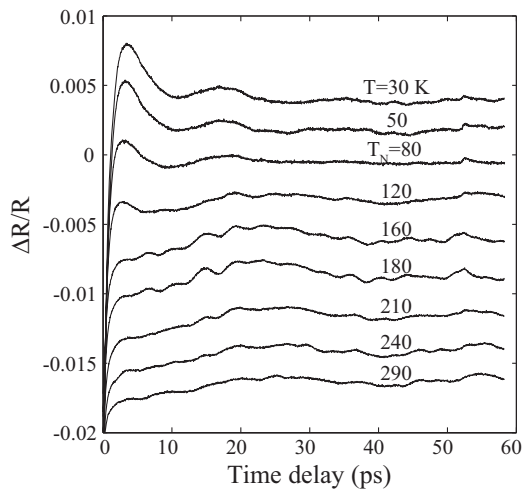

FIG. 2. Photoinduced reflectance change $\Delta R(t)/R$ plotted as a function of time-delay for various temperatures. The reflectivity data are shifted along the vertical axis for clarity.
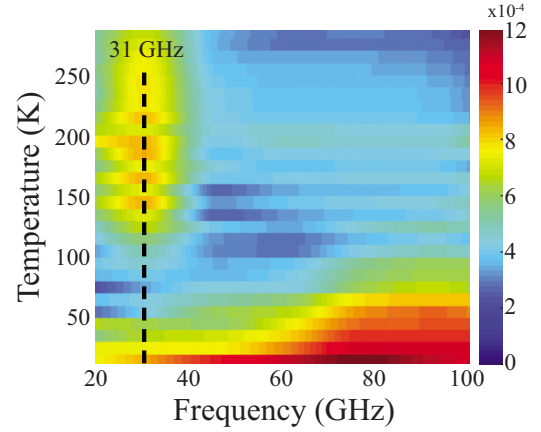

FIG. 3. (Color online) FT amplitudes of coherent oscillation. The dashed line represents the frequency of the high-temperature region.

ingly different frequency responses are clearly observed: one is at the approximately 31 GHz oscillation above T_N, the other is at a higher frequency below T_N (the magnetic ordering phase). The frequency of the 31 GHz oscillation is strongest near $T=190$ K. This coherent oscillation behavior is in good agreement with another previously studied hexagonal multiferroic, $LuMnO_3$ experiment;[7] a coherent mode at 47 GHz was found and assigned as an acoustic phonon mode.

This oscillation is explained as the propagating strained layer mechanism for acoustic phonon generation.[19,20] For a bulk material, a strained layer generated at the surface propagating with an acoustic phonon wave speed v_s such that the interference produced by the probe pulses reflect partially at the surface and also at $z=v_s\tau_d$ (after time delay τ_d), shows an oscillatory behavior. Then, Maxwell's equation for the electric field $E(z,t)$ of the probe pulse under the slowly varying envelope approximation is given as $\partial^2 E(z,t)/\partial z^2 + (\omega_{probe}/c)^2[n_0+\delta n(z,t)]^2 E(z,t)=0$, where ω_{probe} is the center frequency of the probe pulse, n_0 is the index of refraction, and δn is the index change due to the strain. Then, the differential reflectance $\Delta R/R$ for the longitudinal acoustic phonon is given by $\Delta R/R \propto (\omega_{probe}/c)\sin[(2n_0\omega_{probe}/c)v_s t+\varphi]$, where φ is the phase angle. The oscillation period is given as $T=\lambda/(2n_0 v_s)$, where λ is the probe wavelength. To fit the data for the coherent phonon amplitude and decay constants, we used an empirical model, consisting of an oscillatory decay and a simple exponential decay, i.e., $\Delta R(t)/R =Ae^{-\gamma t}\cos(\omega t+\phi)+Be^{-\beta t}+C$, where ω is the angular frequency, γ is the damping constant, and β is the nonoscillatory relaxation rate. The temperature dependence of the phonon amplitudes is plotted in Fig. 4, which is similar to the result of the FT analysis (following the dashed line in Fig. 3).

The acoustic phonon at 31 GHz is the strongest near 190 K and weakens as the temperature approaches T_N. We attribute this behavior to the short range antiferromagnetic correlation above T_N. The acoustic phonon can be strongly coupled to spin fluctuations above and below the T_N according to the thermal analysis of Sharma *et al.*[21] In the high temperature phase, near and above T_N, the interacting spins fluctuate energetically among the nearly degenerate ground state configurations originating from the geometric frustration. Thus, a generic spin coupling to the phonons at the phase transition temperature can cause the significant observed spin-scattering behavior.[22–24]
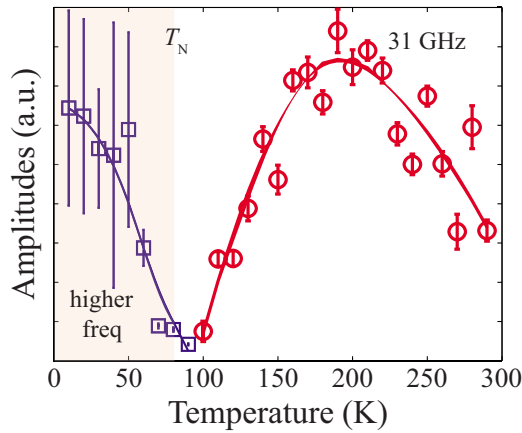
FIG. 4. (Color online) Temperature dependence of the phonon amplitudes obtained by the model analysis using Eq. (3). The phonon amplitude above T_N is plotted in circles, and below T_N in squares. The lines are visual guides.

Additionally, the lattice vibration mode measured in the pump-probe spectroscopy is sensitive to change in the group symmetry. In the ferroelectric phase, the ferroelectric polarization appearing along the *c* axis is caused by the tilting of the MnO_5 polyhedron and the distortion of the Y ions.[10] In the low temperature region, Mn ions begin to align antiferromagnetically in such a way that the magnetic moments are arranged on the *ab*-plane in a 120° structure. Also, the Mn^{3+} (S=2) spins interact antiferromagnetically within the hexagonal layers of the structure, forming a geometrically frustrated magnet. The combined effects of the geometrically frustrated triangular Mn arrangement and the strong two-dimensionality of the magnetic order result in a reduction in the ordered magnetic moment.[8] Thus, the significant change in phonon mode near T_N shown in Fig. 3 can be related to the giant magneto-elastic coupling in the isostructural transition in hexagonal manganites.[25]

In summary, we measured the temperature-dependent behavior of the coherent phonon mode in multiferroic $YMnO_3$ using femtosecond pump-probe differential reflectance spectroscopy. Coherent oscillation of the acoustic modes was found above T_N, showing strong spin-lattice coupling in this multiferroic material. The coherent acoustic phonon dynamics are consistent with the result reported for $LuMnO_3$.[7] The excited $d_{(3z^2-r^2)'}$ electron is responsible for the spin order in this geometrically frustrated magnetic system, and, therefore, by combining these two results together, we attribute the origin of the acoustic phonon generation to magnetic ordering. Our time-domain spectroscopic result, therefore, supports Sharma *et al.*[21] dynamic spin-phonon picture.

[1] N. A. Spaldin and M. Fiebig, Science **309**, 391 (2005).
[2] T. Lottermoser, T. Lonkai, U. Amann, D. Hohlwein, J. Ihringer, and M. Fiebig, Nature (London) **430**, 541 (2004).
[3] N. Hur, S. Park, P. A. Sharma, J. S. Ahn, S. Guha, and S.-W. Cheong, Nature (London) **429**, 392 (2004).
[4] W. Eerenstein, N. D. Mathur, and J. F. Scott, Nature (London) **442**, 759 (2006).
[5] S.-W. Cheong and M. Mostovoy, Nature Mater. **6**, 13 (2007).
[6] H. Yakel, W. C. Koehler, E. F. Bertaut, and F. Forrat, Acta Crystallogr. **16**, 957 (1963).
[7] K.-J. Jang, J. Lim, J. Ahn, J.-H. Kim, K.-J. Yi, J. S. Ahn, and S.-W. Cheong, New J. Phys. **12**, 023017 (2010).
[8] A. Muñoz, J. A. Alonso, M. J. Martinez-Lope, M. T. Casais, J. L. Martinez, and M. T. Fernandez-Diaz, Phys. Rev. B **62**, 9498 (2000).
[9] M. N. Iliev, H.-G. Lee, V. N. Popov, M. V. Abrashev, A. Hamed, R. L. Meng, and C. W. Chu, Phys. Rev. B **56**, 2488 (1997).
[10] T. Katsufuji, M. Masaki, A. Machida, M. Moritomo, K. Kato, E. Nishibori, M. Takata, M. Sakata, K. Ohoyama, K. Kitazawa, and H. Takagi, Phys. Rev. B **66**, 134434 (2002).
[11] B. B. Van Aken and T. T. M. Palstra, Phys. Rev. B **69**, 134113 (2004).
[12] D. G. Tomuta, S. Ramarkrishnan, G. J. Nieuwenhuys, and J. A. Mydosh, J. Phys.: Condens. Matter **13**, 4543 (2001).
[13] A. B. Souchkov, J. R. Simpson, M. Quijada, H. Ishibashi, N. Hur, J. S. Ahn, S. W. Cheong, A. J. Millis, and H. D. Drew, Phys. Rev. Lett. **91**, 027203 (2003).
[14] S. Lee, A. Pirogov, J. H. Han, J.-G. Park, A. Hoshikawa, and T. Kamiyama, Phys. Rev. B **71**, 180413(R) (2005).
[15] R. D. Averitt and A. J. Taylor, J. Phys.: Condens. Matter **14**, R1357 (2002).
[16] K. Lukaszewicz and J. Karut-Kalicinska, Ferroelectrics **7**, 81 (1974).
[17] A. V. Kimel, R. V. Pisarev, F. Bentivegna, and T. Rasing, Phys. Rev. B **64**, 201103(R) (2001).
[18] T. Katsufuji, S. Mori, M. Masaki, Y. Moritomo, N. Yamamoto, and H. Takagi, Phys. Rev. B **64**, 104419 (2001).
[19] C. Thomsen, H. T. Grahn, H. J. Maris, and J. Tauc, Phys. Rev. B **34**, 4129 (1986).
[20] R. Liu, G. D. Sanders, C. J. Stanton, C. S. Kim, J. S. Yhang, Y. D. Jho, K.-J. Yi, E. Oh, and D. S. Kim, Phys. Rev. B **72**, 195335 (2005).
[21] P. A. Sharma, J. S. Ahn, N. Hur, S. Park, S. B. Kim, S. Lee, J.-G. Park, S. Guha, and S.-W. Cheong, Phys. Rev. Lett. **93**, 177202 (2004).
[22] K. Kawasaki, Prog. Theor. Phys. **29**, 801 (1963).
[23] F. B. Lewis and N. H. Saunders, J. Phys. C **6**, 2525 (1973).
[24] Y. K. Tsui, C. A. Burns, J. Snyder, and B. Schiffer, Phys. Rev. Lett. **82**, 3532 (1999).
[25] S. Lee, A. Pirogov, M. Kang, K.-H. Jang, M. Yonemura, T. Kamiyama, S.-W. Cheong, F. Gozzo, N. Shin, H. Kimura, Y. Noda, and J.-G. Park, Nature (London) **451**, 805 (2008).